

Microfibrous nickel substrates and electrodes for battery system applications

Wenhua H. Zhu^{*}, Peter J. Durben, Bruce J. Tatarchuk

Department of Chemical Engineering, Center for Microfibrous Materials Manufacturing, Auburn University, Auburn, AL 36849, USA

Received 2 May 2002; accepted 14 May 2002

Abstract

The use of microfibrous nickel substrates is advantageous for increasing the surface area available for the deposition of active material and reducing the substrate weight and consequently, yields a higher specific capacity for nickel hydroxide electrodes. Porous, microfiber-based nickel substrates were produced by sintering a composite preform. The preforms, consisting of nickel fibers with diameters as small as 2 μm and cellulose fibers, were formed using a papermaking process. The fabricated nickel electrodes that included a supporting nickel mesh in the substrate tested in a 26% KOH half-cell delivered a specific capacity of more than 250 mAh/g of the electrode weight (i.e. fibrous substrate, nickel mesh, and active material) at a 1.0 C discharge rate. An Auburn electrode without a nickel mesh tested in the same half-cell attained a higher specific capacity of 268 mAh/g at a 1.37 C discharge rate. The substrates used in these electrodes had porosities of 95–97%, and greatly improved the specific capacity of the nickel electrode. With the use of the microfibrous electrode, improved specific energies of nickel-based cell and battery designs are possible. When assembled in a nickel–hydrogen (Ni–H₂) boilerplate cell, the specific capacity of nearly 230 mAh/g was observed for the nickel electrode at a 0.5 C rate during the 127th cycle test. The results of high specific capacity and quick rise in utilization of microfibrous nickel hydroxide electrodes make these electrodes good candidates for significantly improving the energy density and performance of nickel–hydrogen cells.

© 2002 Elsevier Science B.V. All rights reserved.

Keywords: Microfibrous substrate; Nickel oxide batteries; Nickel hydrogen cells

1. Introduction

The nickel electrode is the positive electrode in several secondary battery systems, such as the nickel–iron, nickel–cadmium, nickel–zinc, nickel–hydrogen (Ni–H₂), and nickel–metal hydride batteries. These batteries find applications in many fields. In the aerospace industry where high performance and reliability in combination with minimum weight are required, nickel–hydrogen batteries are often the system of choice. Since the nickel electrode in this system has been shown to be the limiting factor in terms of performance and weight [1,2], work has focused on improving the nickel electrode. Much of this work has been directed toward developing alternative electrode microstructures and devising effective methods of loading and distributing the active material into the collector matrix.

Research has focused on improving the specific capacity of the nickel electrode. Current state-of-the-art (SOA) nickel

electrodes made with a sintered nickel powder substrate typically have specific capacities of 105–120 mAh/g. In 1993, Lim and Zelter [3] produced nickel electrodes using 90% porous Fibrex[®] fiber-powder substrates which demonstrated a higher usable specific capacity (ca. 130 mAh/g in 26% KOH) than that of SOA nickel electrodes. Then in 1995, they increased the specific capacity by about 20% to 147 mAh/g after 327 cycles using 88% porous and 1.52 mm thick Fibrex[®] fiber based substrates [4]. Taucher et al. produced electrodes in 1996 with specific capacities of 133–145 mAh/g by using FN090 nickel felt from Sorapec (France) [5]. That same year, Rouget et al. developed a three-dimensional substrate with two woven faces interconnected by fibers, and nickel electrodes made with this substrate obtained specific capacities of 164–169 mAh/g [6].

The highest reported specific capacities have been with electrodes made from microfibrous substrates. In 1995, Britton reported a specific capacity of 195 mAh/g with 2 μm diameter nickel fiber electrodes developed at Auburn University [7]. Lightweight and high specific capacity nickel electrodes developed by Eagle–Picher in 1996 delivered in excess of 180 mAh/g, but did not surpass that reported by

^{*} Corresponding author. Tel.: +1-334-844-2025; fax: +1-334-844-2085.
E-mail address: whzhu@eng.auburn.edu (W.H. Zhu).

Britton the previous year [8]. These nickel electrodes were based on a highly porous, nickel microfiber (<10 μm diameter) substrate.

Besides the high specific capacity, microfibrillar based electrodes exhibited high initial utilization.¹ Lightweight nickel fiber electrodes previously made from nickel fibers with a larger diameter (25 μm) had a common problem of exhibiting a low initial utilization, which gradually increased with cycling [9]. The use of the smaller fibers improves initial utilization [10]² due to the substrate's large surface area and an increase in electrochemical accessibility to the active material [11].

Further, development by Adanuvor et al. of the previously mentioned Auburn electrode indicated that even higher specific capacities might be possible. Their electrodes were based on a highly porous substrate consisting of 2 μm diameter nickel fibers [12].

An effective substrate provides a supporting structure to house the active material while also providing a low resistant current conducting pathway between the active material and the cell terminal. In this paper, fabrication of microfibrillar substrates and nickel hydroxide electrodes based on these substrates is introduced. The microstructural features of sintered fibrous substrates are presented, and the applications of the microfibrillar substrate in nickel hydroxide electrodes and nickel–hydrogen cells are also discussed.

2. Experimental procedure

2.1. Forming process of preforms and substrates

Using Auburn University patented technologies [14,15,28], 2, 8, and/or 12 μm diameter nickel fibers (Memetec America Corporation, chopped 3.18 mm in length) along with 50 w/o cellulose fibers were agitated in 1 L of water for 5–20 min. The dispersed fiber mixture was then gathered on a sheet mold (16.0 cm in diameter) to form a wet paper composite preform. The preform was pressed at ca. 400 kN/m² twice, and then dried at 60 C for 24 h. A nickel mesh (0.03 mm in thickness) was used as a current collector for some samples and was located in the middle of two separate preform sheets. The paper preforms were sintered in a quartz tube with hydrogen flowing through the reactor. Large preforms were also sintered in a continuous belt furnace at 950–1100 C in a hydrogen reducing atmosphere. During sintering, the small nickel fibers fuse together at their contact points to form an interlocking metal network. The substrates were ultrasonically washed with deionized water. This was followed by a wet oxidation cleaning treatment to minimize corrosion during the impregnation process [16].

¹The commonly used term of utilization is a useful parameter for approximately monitoring the actual use of active material in the nickel electrode during the cycling process (Section 2.3).

²Computer program caused the utilization error. It was fixed by Adanuvor et al. [12].

2.2. Impregnation of microfibrillar substrates

The substrates were impregnated with nickel hydroxide active material using an electrochemical impregnation technique. The aqueous impregnation solution consisted of 2 M Ni(NO₃)₂, 0.23 M Co(NO₃)₂, and 0.10 M NaNO₂. The electrochemical impregnation procedure was conducted in a water-jacketed beaker (700 ml solution) maintained at 90 \pm 1 °C. The pH of the solution was initially adjusted to the desired value of 4 by adding ammonium hydroxide. The microfibrillar substrate was placed between two nickel foils (0.07 mm in thickness) that served as anodes. A piece of nickel wire was spot-welded to the substrate for use as a lead connection to the power supply. The substrates were impregnated using multiple current steps until the desired loading level, between 1.1 and 2.0 g/cm³ void, was obtained. After impregnation, each electrode was rinsed in deionized water, then dried at 70 C for 2 h. Two electrodes (TED109 and TED110) were further post-impregnated in a 1.8 M Co(NO₃)₂ solutions for 20 min then dried [17]. All electrodes were then soaked in 26% KOH for 4 h then formed using eight cycles of 20 min charge and 20 min discharge at a 70 mA/cm² current density in 26% KOH solution. The formed electrodes were washed in deionized water until the pH value of the washing solution was neutral, dried at 60 C for 4 h, and weighed. The theoretical capacity of the formed nickel electrodes was determined from the weight gain of the substrate and the electrochemical equivalent of 289 mAh/g of nickel hydroxide. The current at various charge and discharge rates was calculated using the theoretical capacity.

2.3. Utilization and specific capacity

Specific energy and power usually describes the performance of a cell or battery. For a formed or cycled nickel electrode, the specific capacity (mAh/g of electrode) is appropriate to evaluate the feature of the electrode. Utilization of active material usually means the ratio of the measured capacity to the theoretically calculated capacity based on the weight of the active material deposited in the substrate. The theoretical capacity (289 mAh/g of active material, Ni(OH)₂) is obtained by assuming one electron is involved in the reaction between β -Ni(OH)₂ and β -NiOOH, i.e. $n_{\beta,\beta} = 1.0$. It is common to consider the active material utilization as 100%. However, the phase cycling between α -Ni(OH)₂ and γ -NiOOH appears to have at least 1.5 electrons involved in the transfer [25], i.e. $n_{\alpha,\gamma} \geq 1.5$. Moreover, the phase cycling between β -Ni(OH)₂ and γ -NiOOH [26] reveals that the number of electron transfer is $1.0 < n_{\beta,\gamma} < 1.3$. In the present work, the term of utilization follows the commonly used definition ($n_{\beta,\beta} = 1.0$) to evaluate the use of active materials during the formation and cycling process. If the utilization rate is over 100%, multiple electron transfer has happened in the reaction between different crystalline phases. If the value is <100%, it shows

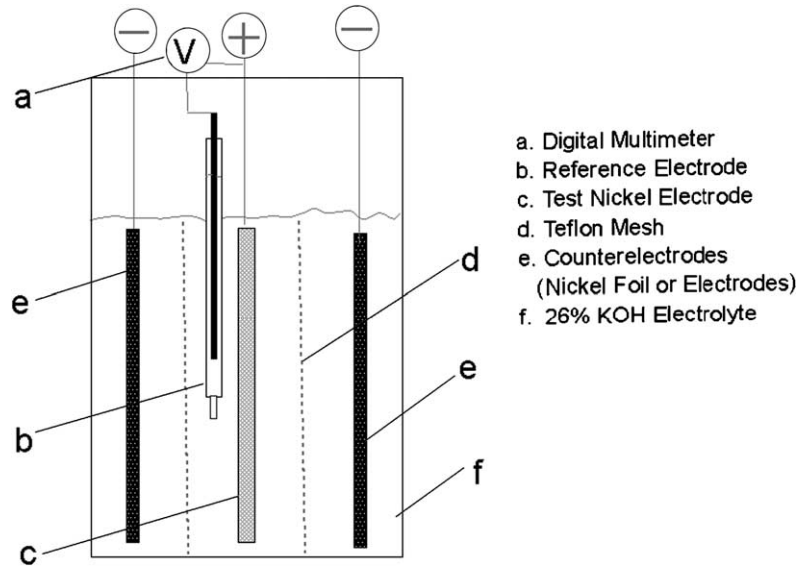


Fig. 1. Schematic diagram of the flooded half-cell test for microfibrous nickel electrodes.

that part of the active material is not activated. As a whole, utilization of active material is a proper parameter to approximately monitor the actual use of active material.

The half-cell for testing is shown schematically in Fig. 1. Before cycling, electrodes were initially soaked in a 26% KOH solution overnight. The cycling test in the flooded cell was carried out using an accelerated low earth orbit (LEO) regime protocol. This consisted of 55 min charge at a 1.1 C rate and 35 min discharge at a 1.37 C rate. After charging at a 1.0 C rate for 80 min, the capacity was measured at a 0.5 C rate to 0.8 V versus a Cd/Cd(OH)₂ reference electrode. The electrode specific capacity in mAh/g was determined from

the measured capacity and the initial weight of the dry electrode after formation, excluding the weight of the spot-welded tab. Both the formation and cycle tests were carried out using a Model 273 EG&G Potentiostat/Galvanostat or a Model BT-2402 Arbin Battery Test System.

2.4. Nickel–hydrogen (Ni–H₂) cells

Two microfibrous nickel hydroxide electrodes were individually assembled in nickel–hydrogen boilerplate cells. The illustration of the monopolar cell used is shown in Fig. 2. The cell consisted of one microfibrous nickel

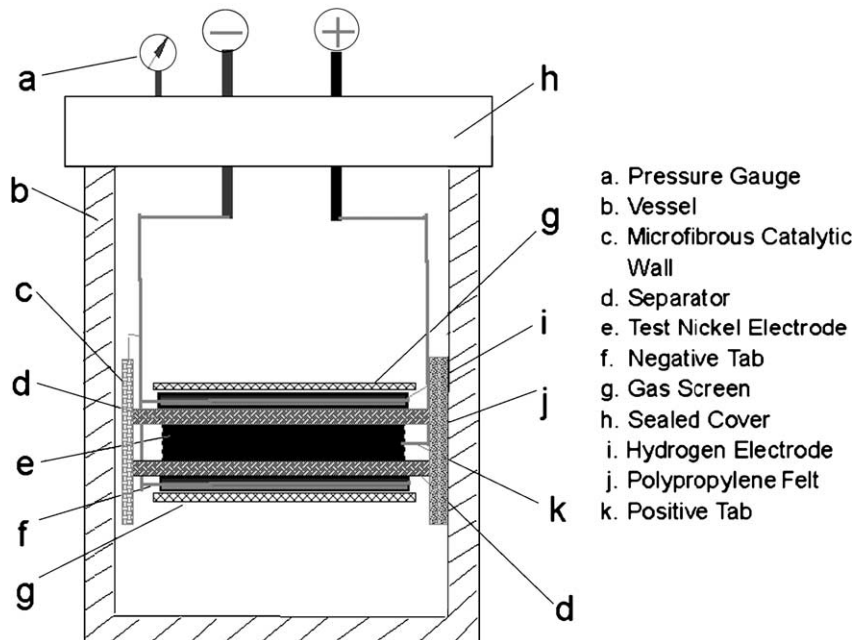


Fig. 2. Illustration of the nickel–hydrogen boilerplate cell.

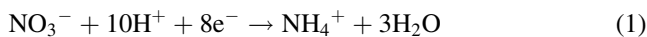
electrode and two hydrogen electrodes with platinum catalyst (0.5 mg/cm^3) (item 16-ESN-HANIBP, Electrosynthesis Co. Inc.). Each electrode was a 2 in. diameter disk. Teflon meshes were used as gas screens. Nickel tabs were welded to the nickel screens of both hydrogen electrodes and the microfibrinous nickel electrode. Three layers of Zircar (Zircar Products Inc.) with serrated edges served as separators and were kept in physical contact with wall wicks for electrolyte management. Polypropylene felts were used as an electrolyte reservoir and wall wicks. A thin microfibrinous nickel substrate was used for oxygen recombination along the cell wall.

The assembled monopolar cell was soaked overnight in a vacuum container filled with 26% KOH. The excess electrolyte was removed before the cell stack was put into the boilerplate pressure vessel. The vessel was first evacuated then filled with hydrogen gas to a stabilized pressure of 50 psi. The cell capacity was measured at a 0.5 C rate after charging at a 1.0 C rate for 80 min. The LEO regime protocol was used during cycling tests.

3. Results and discussion

3.1. Reactions for deposition of nickel hydroxide

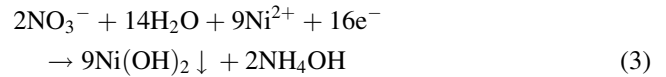
Electrochemical impregnation is the method of choice for introducing active material into microfibrinous substrates. This method is based on a nitrate reduction process in which the microfibrinous substrate is cathodically polarized in a bath of aqueous nickel nitrate solution. Kandler [18] proposed that the deposition within the pores of the substrate is brought about by a pH increase during NO_3^- reduction. Hausler [19] quantitatively confirmed that NH_4^+ ions are produced according to the cathodic reaction



At higher current densities of 10, 30, and 60 mA/cm^2 , Takamura et al. [20] revealed that the amount of NH_4OH is proportional to the amount of input charge according to the reaction



Ho and Jorne [21] modified the mechanism by Kandler for use with alkaline solutions and acquired the overall cathodic reaction



It is assumed here that the precipitation of $\text{Ni}(\text{OH})_2$ is carried out according to reaction (3). Process parameters such as temperature, solution concentrations, current densities, and pH need to be precisely chosen in order to obtain a desired loading level. By manipulating these parameters, it is possible to precipitate nickel hydroxide in a uniform coat directly on the fiber surface, as opposed to in the void spaces between the fibers. This allows for shorter transport distances for diffusing species in the active material layer and greater accessibility of active material to the electrolyte in the void spaces. This makes possible an improved electrode at a lighter weight.

3.2. Parameters of paper preform and microfibrinous substrate

Preform composition and substrate parameters are given in Table 1. Preforms, substrates, and electrodes were examined using scanning electron microscopy (SEM) in order to view structure features. The larger cellulose fibers shown in Fig. 3a were employed as a binder to form the paper preform in the manufacturing process. Upon sintering, a void volume was produced when the cellulose gasified, and the small nickel fibers “micro-welded” at their contact points to form an interlocking metal network. As shown in Fig. 3b and c, the resulting three-dimensional network structure with characteristics of high surface area, low weight, and favorable electrical conductivity can be used for improving the specific capacity of the nickel hydroxide electrode. The structure after formation and cycle testing is shown in Fig. 3d.

The highly porous microfiber materials have a lower weight and higher surface area than the typical heavy-sintered powder or large diameter fibrous support materials, as shown in Table 2. In comparison with the heavy-sintered nickel powder plaque (80% porosity, 1.8 g/cm^3), the micro-

Table 1
Preform composition and parameters of sintered microfibrinous nickel substrates

Number of substrate	Before sintering				After sintering		
	Percent preform composition				Thickness (mil)	Porosity (%)	Area dimensions
	2 μm	8 μm	12 μm	Cellulose			
151	22.2	0	27.8	50	54	93	2 in. disc
213	50.0	0	0	50	55	97	1 in. \times 2 in.
219	52.7	23.6	14.6	9.1	57	94	2 in. disc
220	52.7	23.6	14.6	9.1	57	94	2 in. disc
221	52.7	23.6	14.6	9.1	57	94	2 in. disc

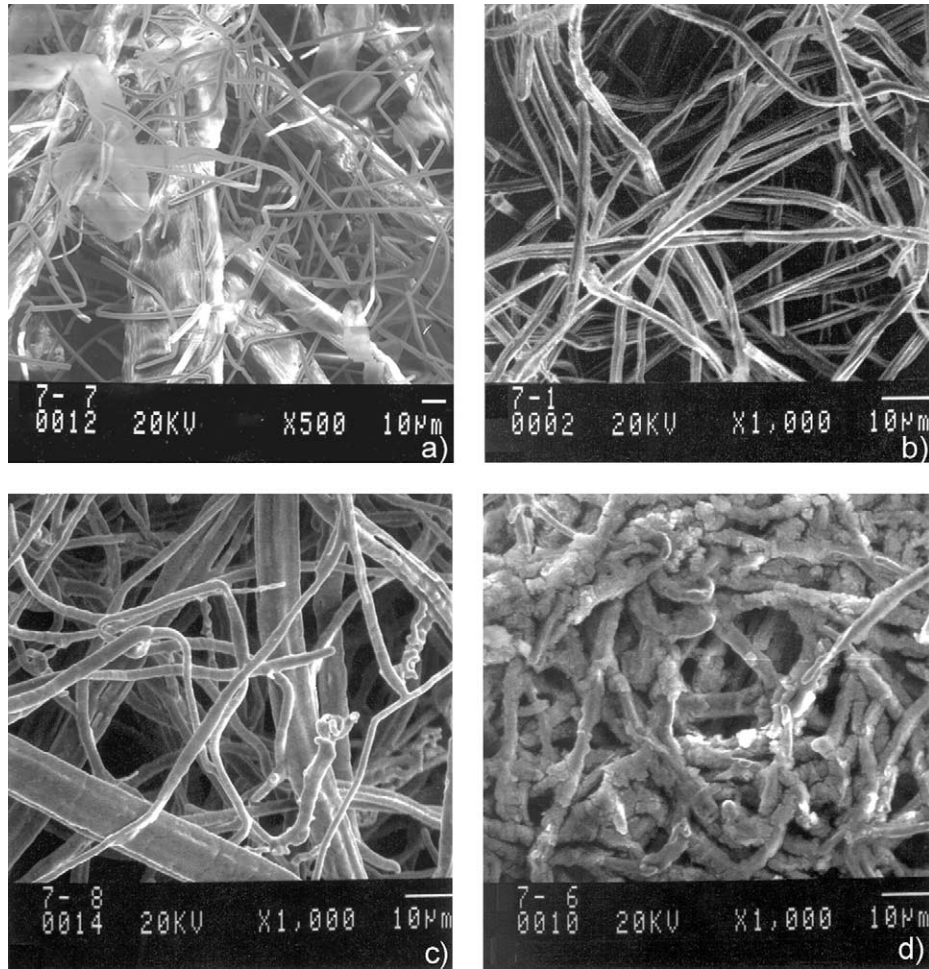


Fig. 3. Scanning electron micrographs of (a) paper preform, (b) micro-welded structure of 2 μm nickel fibers, (c) microfibrinous substrate made from the mixture of 2, 8, and 12 μm nickel fibers, and (d) formed and cycled nickel hydroxide electrode.

fibrous substrate (94% porosity, $\sim 0.55 \text{ g/cm}^3$) is about 70% lighter in weight. Microfibrinous substrates of 97% porosity made from 2 μm diameter nickel fiber have a calculated surface area of $562 \text{ cm}^2/\text{cm}^3$. This is approximately three times higher in surface area than 90% porous Fibrex[®] material ($200 \text{ cm}^2/\text{cm}^3$). Due to these features, the theoretical capacity of the nickel hydroxide electrode made from the higher surface area and lighter weight microfibrinous substrate increased to more than 200 mAh/g, as indicated in Table 3. The utilization of active material for

this electrochemically impregnated electrode is typically 120% [22]. Therefore, it is possible to obtain a high specific capacity in nickel-based cells by incorporating this type of microfibrinous electrode.

3.3. Comparison of initial cycle performance of nickel electrodes

Several paper preforms and substrates have been tested to obtain nickel electrodes with high specific capacity,

Table 2
Three-type of porous metal materials for nickel hydroxide electrodes

Porous sintered nickel materials	Fiber/or powder diameter (μm)	Porosity (%)	Weight (g/cm^3)	Surface area (cm^2/cm^3)	Weight advantage (%)
Auburn microfibrinous substrate ^a	2	97	0.24	562	86.7
	2	95	0.5	1170	72.2
Fibrex [®] metal fiber material ^b	20	90	0.8	200	55.6
Powder sintered nickel plaque ^c	2	80	1.8	4000	0

^a Porosity of the microfibrinous substrate is calculated from the ratio of the void volume to the total volume of the substrate.

^b National Standard Company, Niles, Michigan.

^c A state-of-the-art plaque is made from INCO255 powder. Data is adapted from [13].

Table 3
Feature parameters of microfibrinous substrates and nickel hydroxide electrodes

Electrode number	Electrode weight (g)	Loading level (g/cm ³ void)	Theoretical specific capacity (mAh/g)
TED151	5.1380	1.52	209.0
TED213	2.3910	1.16	238.8
TED219	7.2188	2.00	219.0
TED220	7.0456	1.63	215.7
TED221	6.0683	2.00	223.4

Table 4
Feature parameters of Auburn microfibrinous substrates and its electrodes

Number of electrode	Microfibrinous substrates		Microfibrinous nickel electrodes		
	Thickness (mm)	Porosity (%)	Electrode weight (g)	Loading level (g/cm ³ void)	Theoretical specific capacity (mAh/g)
TED103	1.80	94	1.5395	1.73	219.7
TED108	1.78	95	1.5365	1.77	222.3
TED109	1.82	94	1.6672	1.86	218.1
TED110	1.68	95	1.3353	1.57	213.4
TED213	1.40	97	2.3910	1.16	238.8

Coulombic efficiency, and energy efficiency. The main parameters are shown in Table 4. The porosity of the nickel substrate is one factor affecting the specific capacity of the battery. When replacing the nickel electrode made from an 80% porous SOA plaque with a 93% Fibrex[®] plaque of the same 0.76 mm thickness and 1.8 g/cm³ void loading level, the calculated specific energy increased by 20% in a 48 Ah nickel–hydrogen cell [23]. The technology of the Auburn fiber microstructure was applied to acquire a relatively uniform porous substrate. Tests of electrodes made with 2 μ m diameter microfiber substrates showed a higher

utilization of active material in comparison to Fibrex[®] fiber electrodes due to the microfiber substrates' higher surface area (2340 cm²/g) and better pore size distribution (20–45 μ m) [11,24]. For the TED110 electrode, the utilization of the active material including the post-addition of cobalt hydroxide was approximately 120% after the 40th cycle (Fig. 4).

Note that the utilization for the three electrodes (TED109, TED110, and TED213) reached 100% or more after the 10th cycle. The report on Fibrex[®] nickel electrodes (0.76 mm, 93% porosity, and 1.80 g/cm³ void loading;

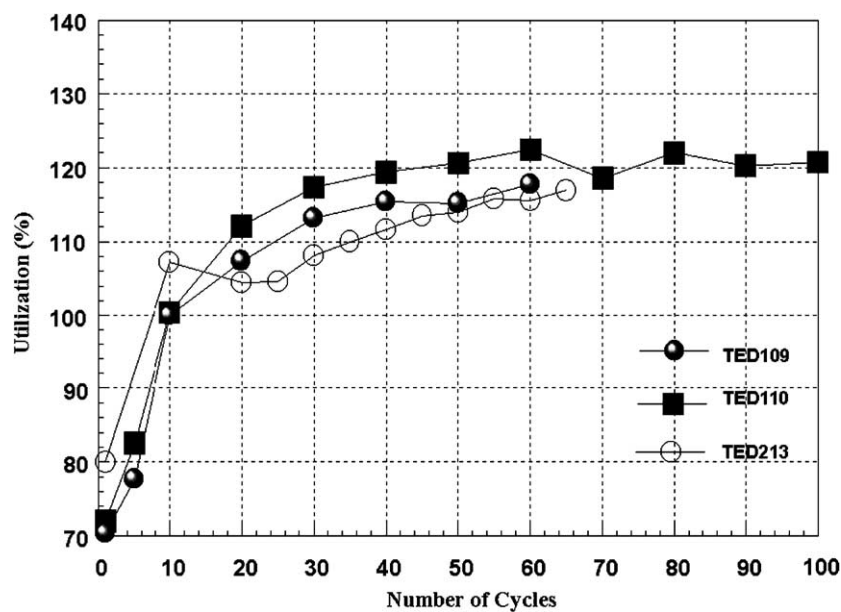


Fig. 4. Utilization vs. number of cycles for microfibrinous nickel electrodes in a LEO cycle regime. Cycle charge: 1.1 C for 55 min. Cycle discharge: 1.37 C for 35 min. Capacity: charge at 1.0 C for 80 min and discharge at 0.5 C to 0.8 V vs. a Cd/Cd(OH)₂ reference electrode.

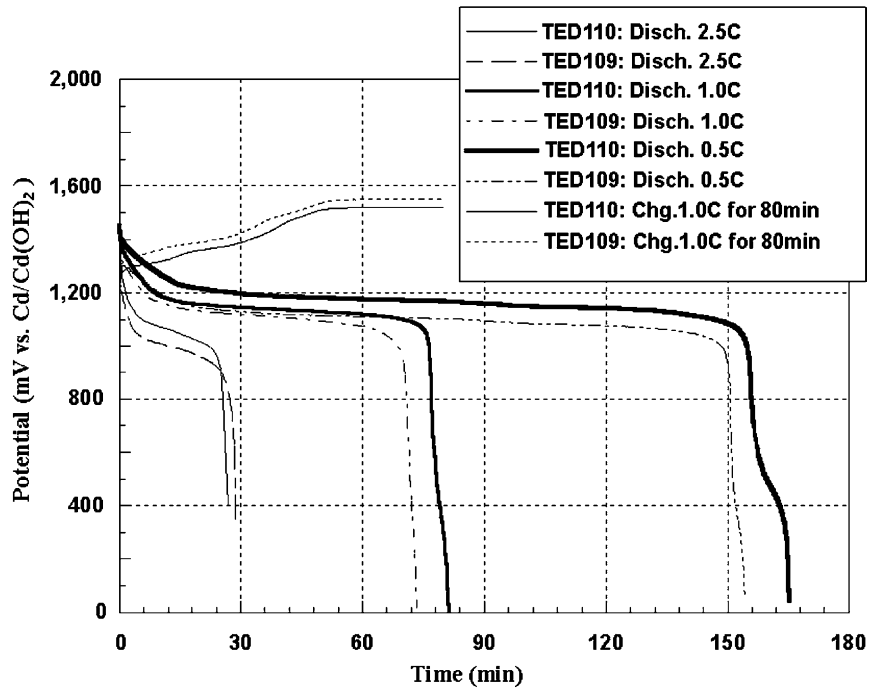


Fig. 5. Charge and discharge curves for microfibrinous nickel electrodes at different discharge rates. Charge: 1.0 C for 80 min.

or 2.0 mm, 90% porosity, and 1.80 g/cm^3 void loading) revealed that it takes more than five hundred cycles to attain 100% utilization in the same cycling conditions [24]. This is attributed to the different microstructure and pore size distribution within the substrates. The Auburn electrodes, on the other hand, have high utilization of active material and show a quick rise towards their theoretical full capacity.

3.4. Rate performance and specific capacity of microfibrinous nickel electrodes

The effects of discharge potentials and discharge rates on the utilization of the active material are shown in Fig. 5 and Table 5, respectively. These show that the TED110 electrode with a lower loading level had better discharge performance. While the electrode still obtained a higher

Table 5

Specific capacity and rate capability of microfibrinous nickel electrodes made from microfibrinous substrates in 26% KOH half-cells

TED109		Utilization (%)	Specific capacity (mAh/g)	TED110		Utilization	Specific capacity
Cycle	Discharge rate (C)			Cycle	Discharge rate (C)		
Microfibrinous nickel electrodes in flooded half-cells							
60	0.5	117.8	257.0	60	0.5	122.5	261.4
61	1.0	116.0	253.1	52	1.0	119.2	254.4
62	1.5	112.9	246.2	63	1.5	110.9	236.8
63	2.0	109.1	237.9	62	2.0	107.9	230.2
64	2.5	106.9	233.1	61	2.5	98.5	210.0
TED213				TED219			
9	0.5	107.2	256.0	63	1.37	96.1	210.5
29	0.5	108.1	258.3	154	2.0	97.8	214.2
30	1.37	103.8	248.0	155	1.37	102.9	225.3
64	0.5	116.9	279.1	156	1.0	103.4	226.5
65	1.37	112.0	267.5	157	0.5	105.8	231.6
TED151				TED220			
Nickel electrodes in nickel–hydrogen cells made from fiber-mixed substrates							
150	2.0	93.4	195.4	124	2.0	96.3	207.6
151	1.37	94.4	197.3	125	1.37	99.9	215.5
152	1.0	95.8	200.3	126	1.0	103.1	222.3
153	0.5	98.9	206.7	127	0.5	106.4	229.4

Table 6
Three types of electrochemical impregnation solutions

Type	Electrochemical impregnation solutions	Electrode number
EIS-1	2.0 M Ni(NO ₃) ₂ , 0.23 M Co(NO ₃) ₂ , and 0.10 M NaNO ₂	151, 213
EIS-2	1.6 M Ni(NO ₃) ₂ , 0.18 M Co(NO ₃) ₂ , and 0.08 M NaNO ₂	219, 220
EIS-3	Previous EIS-1 impregnating solution, the solution density is adjusted to the same as that of the EIS-2 solution	221

discharge potential at a 2.5 C discharge rate, its utilization reduced from 122.5% at a 0.5 C discharge rate to 98.5% at a 2.5 C discharge rate. During normal cycling (a LEO regime with 55 min charge and 35 min discharge at 80% DOD), the Coulombic and energy efficiencies were 78.9% and 63.0%, respectively. The energy efficiency of the TED109 electrode was only 49.0%. This was due to a lower discharge voltage resulting from higher Ohmic resistance in the tab and wires and the heavy loading level.

The specific capacity and rate capability values are shown in Table 5. The weight of active material increased approximately by 1.67% in comparison with the original weight of the formed electrode. The values in Table 5 neglected this small change in weight. The typical specific capacity (ca. 120 mAh/g) of the SOA sintered powder electrode is 41.5% of the theoretical value. The specific capacity of a Fibrex[®] nickel electrode made from an 88% porous substrate was 147 mAh/g of electrode weight after 327 cycles, which is 50.9% of the theoretical value [4]. The specific capacity of nickel electrodes made from 90% Sorapec nickel felt was 133–145 mAh/g of electrode weight, which is 46.0–50.2% of the theoretical value [5]. Also, A nickel fiber (<10 μm in diameter) electrode made by Eagle–Picher had a specific

capacity of 180 mAh/g, which is 62.3% of the theoretical value [8].

The TED109 nickel electrode discharged at 1 h rate attained a specific capacity of 253.1 mAh/g on the 61st cycle. This is 87.6% of the theoretical value. The TED110 nickel electrode discharged at 1 h rate attained a specific capacity of 254.4 mAh/g on the 52nd cycle. This is 88.0% of the theoretical value. And the TED213 electrode discharged at 1.37 C rate attained a specific capacity of 267.5 mAh/g on the 65th cycle. This is 92.6% of the theoretical value. The Auburn microfibrous nickel electrode had a significantly higher specific capacity over other nickel electrode designs. With its use, a significant increase in the specific energy of nickel-electrode-limited sealed cells and batteries is possible. This is especially beneficial for aerospace nickel–hydrogen battery applications.

The utilization of active material in the microfibrous nickel electrodes made from three different impregnation solutions (Table 6) is shown in Fig. 6. The TED213 nickel electrode had a loading level of 1.16 g/cm³ void, and the TED219 and TED221 electrodes had a loading level of 2.0 g/cm³ void. The differences in utilization suggest consumption rates of nickel and cobalt ions in the impregnation

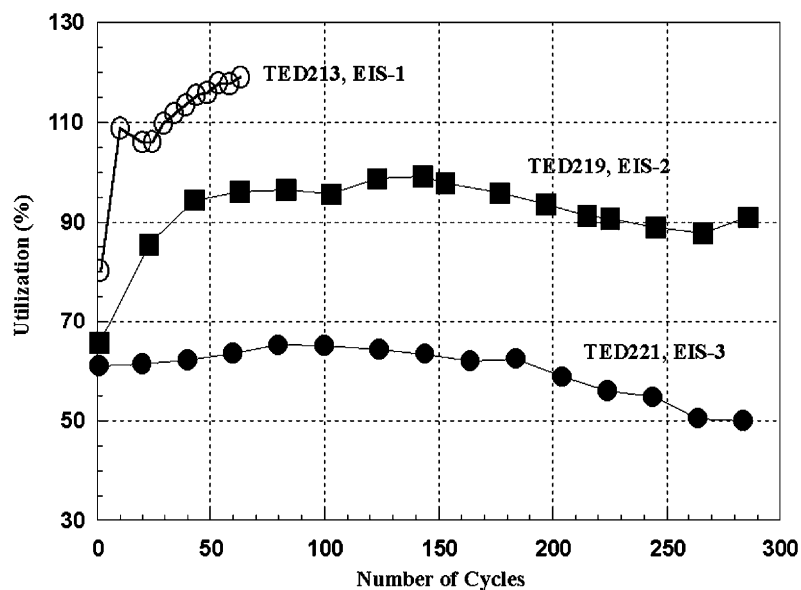


Fig. 6. Utilization vs. number of cycles of microfibrous nickel electrodes in an electrolyte-flooded cell. Electrodes were made in three kinds of impregnation solution as shown in Table 6. Cycle charge: 1.1 C for 55 min. Cycle discharge: 1.37 C for 35 min. Capacity: charge at 1.0 C for 80 min and discharge at 0.5 C to 0.8 V vs. a Cd/Cd(OH)₂ reference electrode.

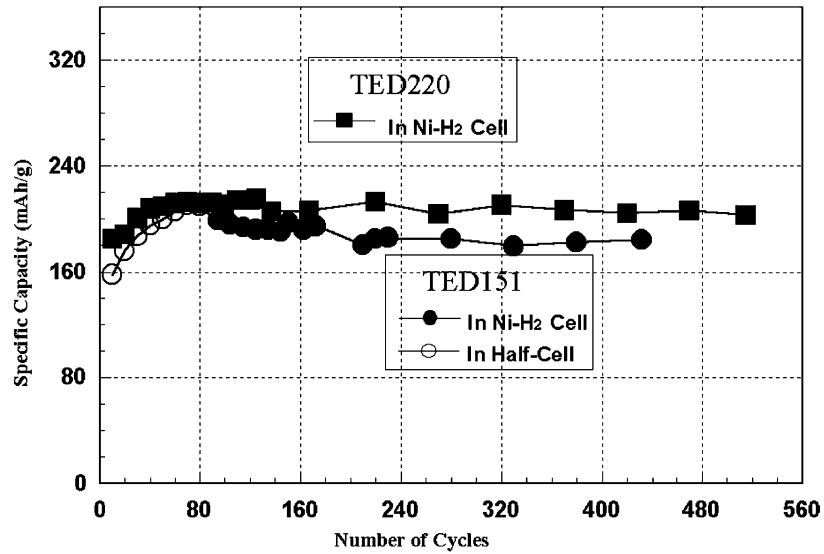


Fig. 7. Specific capacity of the microfibrinous nickel electrodes made from fiber mixture substrate in the nickel–hydrogen cells.

solution may be different. Absorption spectrometry analysis [5] of impregnated nickel electrodes has shown that the content fraction of cobalt in the electrode is higher than the content fraction in the impregnation solution. Cobalt is an important additive for improving utilization of nickel electrodes made from a highly porous microfiber substrate. The lower utilization of the TED221 nickel electrode obtained from EIS-3 solution suggests that the cobalt ions have a higher consumption rate than nickel ions. Solubility of products also demonstrates that cobalt hydroxide has a higher rate of deposition than nickel hydroxide inside the pores (solubility of products, $k_{sp,Co(OH)_2} = 1.6 \times 10^{-15}$, and $k_{sp,Ni(OH)_2} = 2.0 \times 10^{-15}$ [27]). In order to maintain uniform

deposition for continuous manufacturing process, the mole ratio of cobalt to nickel ions should be adjusted to an effective range.

3.5. Applications of microfibrinous nickel electrodes in nickel–hydrogen ($Ni-H_2$) batteries

The utilization of active material in paste type nickel electrodes made with woven metallic substrates was poor at a higher discharge rate (85–88% at a 1.0 C discharge rate) [6]. In comparison, the TED213 electrode made from a substrate containing 2 μm diameter nickel fibers reached a utilization of over 100% by the 9th cycle. These results show

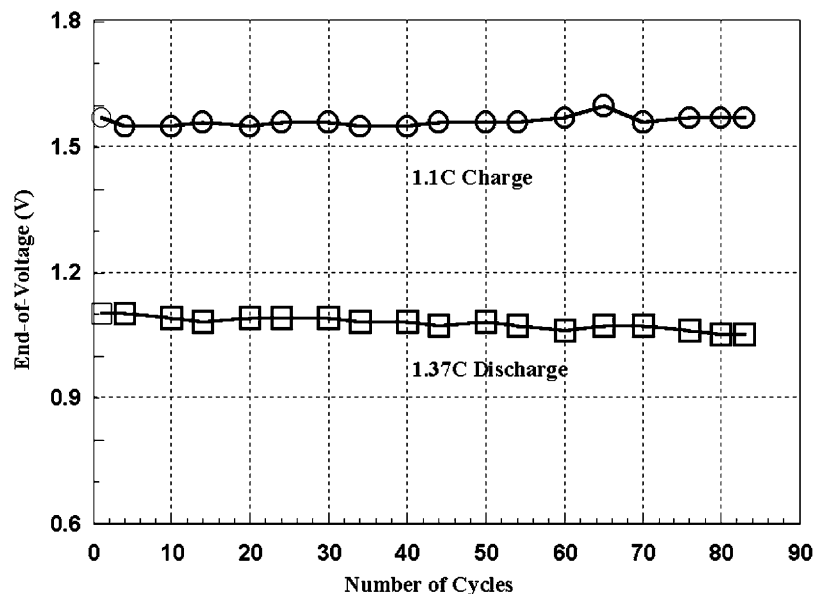


Fig. 8. The end of charge and discharge voltage vs. number of cycles at 80% DOD of nickel–hydrogen cell using the TED151 nickel electrode.

that by using a microfiber-based substrate, there is an improvement in specific capacity and electrode performance over the electrodes made from other commonly used substrates or plaques.

After these encouraging results, the microfiber-based electrodes (TED151 and TED220) were assembled in a nickel–hydrogen boilerplate cell. The substrates used in these electrodes consisted of a 2, 8, and 12 μm diameter fiber mixture, as shown in Table 1. The TED151 nickel electrode was first cycled in a flooded electrolyte cell for 90 cycles in which the utilization at a 0.5 C discharge rate had risen to 100.7%. At this point, the specific capacity was 210 mAh/g of electrode weight. The TED151 electrode after these flooded cycles and the TED220 electrode after formation were separately assembled into the boilerplate cell. The specific capacities of the nickel electrodes are shown in Fig. 7.

After 200 cycles, the stabilized specific capacity of the TED151 nickel electrode was more than 180 mAh/g, and that of the TED220 nickel electrode was more than 200 mAh/g. The specific capacity of the TED220 electrode was higher due to the greater percentage of smaller diameter fibers in the substrate composition and an improvement of the electrolyte management.

The ends of charge and discharge voltages are shown in Fig. 8 for the nickel–hydrogen cell made with the TED151 electrode. With the LEO cycling regime, the end of the charge voltage was from 1.55 to 1.57 V, and the end of discharge voltage was from 1.05 to 1.10 V. These favorable results indicate that by incorporating microfiber-based nickel electrodes in a cell design, specific energy of nickel–hydrogen cells and batteries may significantly improve.

4. Conclusions

The nickel electrode is a limiting factor for a battery's specific energy. But the performance of nickel hydroxide electrodes has improved through new designs. One such improvement is the Auburn microfibrinous electrode. Microfibrinous substrates are a highly porous three-dimensional metallic support for the active material of the nickel hydroxide electrode. This porous substrate has low weight, high surface area, and good electrical conductivity. The microfibrinous nickel electrodes made from 94 to 97% porosity substrates delivered a high specific capacity of 253–268 mAh/g at the 1 h discharge rate or more. The specific capacities are 87.6–92.6% of the theoretical capacity of nickel hydroxide. By incorporating the Auburn nickel electrode in nickel–hydrogen boilerplate cell, the nickel hydroxide electrode made from the substrate attained a specific capacity of nearly 230 mAh/g electrode weight at a 0.5 C rate during the 127th cycle. The quick rise in utilization value is due to the higher surface area of the substrate available for the electrochemical reaction of the active

material. The results of high specific capacity and quick rise in utilization of microfibrinous nickel hydroxide electrodes make these electrodes good candidates for significantly improving the energy density and performance of nickel–hydrogen cells.

Acknowledgements

This project was funded by NASA Lewis Research Center, Electrochemical Technology Branch, Contract #NAS-NAG3-1154. The authors wish to thank Doris L. Britton from NASA Lewis Research Center for her guidance and advice. The authors also wish to acknowledge contributions from Prosper Adanuvor, Johnnie Pearson, Richard Ferro, Bradley Johnson, and Greg Swain during the initial phases of this project.

References

- [1] D.L. Britton, Performance of Lightweight Nickel Electrodes, NASA Technical Memorandum 100958, 1988.
- [2] D.L. Britton, in: D.A. Corrigan, A.H. Zimmerman (Eds.), Nickel Hydroxide Electrodes, Vol. 90 (4), The Electrochemical Society Inc., Pennington, NJ, 1990, p. 234.
- [3] H.S. Lim, G.R. Zelter, *J. Power Sources* 45 (1993) 195.
- [4] H.S. Lim, G.R. Zelter, F.D. Montague, J.J. Smithrick, Effects of Substrates, Their Treatments, and Formation Regimes on Nickel Electrode Performance, IECEC Paper No. AP-371, ASME, New York, 1995, pp. 137–141.
- [5] W. Taucher, T.C. Adler, F.R. McLarnon, E.J. Cairns, *J. Power Sources* 58 (1996) 93.
- [6] R. Rouget, B. Bugnet, R. Lumbroso, in: Proceedings of the 37th Power Sources Conference, Cherry Hill, NJ, 1996, pp. 410–412.
- [7] D.L. Britton, in: Proceedings of the Space Electrochemical Research and Technology Conference, NASA Conference Publication 3337, NASA Lewis Research Center, Cleveland, OH, 1995, p. 8.
- [8] J. Francisco, D. Chiappetti, D. Coates, in: Proceedings of the Annual Battery Conference on Appl. Adv., 11th Edition, IEEE, New York, 1996, p. 141.
- [9] D.L. Britton, Lightweight Fibrous Nickel Electrodes for Nickel–Hydrogen Batteries, NASA Technical Memorandum 101997, 1989.
- [10] B.A. Johnson, R.E. Ferro, G.M. Swain, B.J. Tatarchuk, *J. Power Sources* 47 (1994) 251.
- [11] D.L. Britton, Recent progress in the development of lightweight nickel electrode, in: Proceedings of the Materials Research Society Symposium, Vol. 393, Materials Research Society, 1995, pp. 271–275.
- [12] P.K. Adanuvor, J.A. Pearson, B. Miller, Bruce J. Tatarchuk, D.L. Britton, in: Proceedings of the Space Electrochemical Research and Technology Conference, NASA Conference Publication 3337, NASA Lewis Research Center, Cleveland, OH, May 1995, pp. 11–21.
- [13] H.H. Law, J. Sapjeta, *J. Electrochem. Soc.* 135 (1988) 2418.
- [14] B.J. Tatarchuk, M.F. Rose, A. Krishnagopalan, US Patent 5,102,745 (1992).
- [15] B.J. Tatarchuk, M.F. Rose, A. Krishnagopalan, J.N. Zabasajja, D. Kohler, US Patent 5,080,963 (1992).
- [16] R.L. Beauchamp, D.W. Maurer, T.D. O'Sullivan, US Patent 4,032,697 (1977).
- [17] D.L. Britton, US Patent 6,265,112 (2001).
- [18] L. Kandler, British Patent 917,291 (1963).

- [19] E. Hausler, in: DH Collins (Ed.), *Power Sources*, Vol. 1, Pergamon Press, Oxford, 1966, p. 287.
- [20] T. Takamura, T. Shirogami, T. Nakamura, *Denki Kagaku* 42 (1974) 582.
- [21] K.C. Ho, J. Jorne, *J. Electrochem. Soc.* 137 (1990) 149.
- [22] J.D. Dunlop, G.M. Rae, T.Y. Yi, *NASA Handbook for Nickel–Hydrogen Batteries*, NASA Reference Publication 1314, 1993, pp. 1–10.
- [23] D.L. Britton, in: *Proceedings of the 34th International Power Sources Symposium*, IEEE, New York, USA, 1990, p. 235.
- [24] D.L. Britton, *NASA Technical Memorandum* 105591, 1992.
- [25] P. Oliva, J. Leonardi, J.F. Laurent, C. Delmas, J.J. Braconnier, M. Figlarz, F. Fievet, A. de Guibert, *J. Power Sources* 8 (1982) 229–255.
- [26] B. Bugnet, M.L. Soria Garcia-Ramos, F.P. Joubert, *EP* 1,176,649 (2002).
- [27] J.A. Dean, *Lange’s Handbook of Chemistry*, 12th Edition, McGraw-Hill, New York, 1979, pp. 5–7.
- [28] B.J. Tatarchuk, M.F. Rose, A. Krishnagopalan, *US Patent* 5,304,330 (1994)